PHILOSOPHICAL TRANSACTIONS OF THE ROYAL SOCIETY A MATHEMATICAL, PHYSICAL & ENGINEERING SCIENCES

Earthquakes and Lineament Infrastructure

R. H. Sibson

Phil. Trans. R. Soc. Lond. A 1986 **317**, 63-79
doi: 10.1098/rsta.1986.0025

Phil. Trans. R. Soc. Lond. A **317**, 63–79 (1986)
Printed in Great Britain

Earthquakes and lineament infrastructure

By R. H. Sibson

Department of Geological Sciences, University of California, Santa Barbara, California 93106, *U.S.A.*

'*A further result attending to the disturbances of the surface of the earth has been to produce rents or fissures in the rocks which have been subject to their violent movements, and to convert them into receptacles of metallic ores accessible by the labours of men.*' (Reverend William Buckland *Geology and mineralogy with reference to natural theology*. London: William Pickering (1836).)

Analyses of the nucleation, propagation and stopping of moderate to large earthquake ruptures, coupled with high-precision studies of background and aftershock micro-earthquake activity, are yielding insights into the infrastructure of major transcurrent fault zones within the seismogenic régime. Curvature and echelon segmentation of a principal slip surface within a *ca.* 1 km wide main fault zone appear to exert major controls on the starting and stopping of ruptures. Geometrical irregularities of this kind, transverse to the direction of rupture propagation, may be usefully classified into dilational and antidilational jogs, referring to the area change in the plane defined by the slip vector and the pole to planar segments of the fault. Extensional fracture systems linking echelon fault segments across dilational jogs allow long-term transfer of fault slip, but appear to play an especially important role as kinetic barriers impeding or arresting rapid rupture propagation. In fluid-saturated crust the rapid transfer of slip is opposed by suctions arising from rupture-induced differential fluid pressures. Delayed slip transfer, delineated by intense aftershock activity, may then occur as fluid pressures re-equilibrate. Fossil examples of such linking extensional fracture systems are characterized by multi-episode hydraulic implosion breccias. Dilational zones of this kind may migrate along faults or remain fixed for relatively long time periods. They serve as particularly favourable sites for hydrothermal mineralization and may also localize magmatic activity along major lineaments.

1. Introduction

The infrastructure of fault zones within the shallow, brittle crust and the geometry of individual fault surfaces has long been of practical concern to geologists, especially within the mining industry (Newhouse 1942; McKinstry 1948). In recent years this interest in fault zone complexity has extended to the seismological community. Detailed mapping of the surface rupture traces produced by shallow earthquakes (Ambraseys 1970; Brown 1970; Tchalenko & Ambraseys 1970; Vedder & Wallace 1970; Clark 1972; Tchalenko & Berberian 1975; Berberian *et al.* 1984), and of mining-induced fault systems (Gay & Ortlepp 1979) has shown them to consist of discontinuous multiple fractures, characteristically showing echelon segmentation on a range of scales (Segall & Pollard 1980). Abrupt changes in the magnitude of fault slip may also occur from one rupture segment to the next (Tchalenko & Berberian 1975; Sieh 1978; Deng & Zhang 1984). Moreover, high-resolution micro-earthquake studies, wherein events are located to relative precisions of under 1 km (Lee & Stewart 1981), have demonstrated that irregularities observed in the surface rupture traces often extend throughout the

seismogenic régime to depths of 10 km or more (Eaton *et al.* 1970; Bakun *et al.* 1980; Reasenberg & Ellsworth 1982). Over about the same period, mathematical models of fault 'barriers' (Das & Aki 1977), 'asperities' (Kanamori 1978; McGarr 1981), 'ligaments' (Rudnicki & Kanamori 1981) and 'roughness' (Nur & Israel 1980) have been devised to account for complexities in seismic waveforms arising from unsteady rupture propagation (Kanamori & Stewart 1978), and for the statistical distribution of different-sized earthquakes (Hanks 1979).

An important related discovery has been the recognition from palaeoseismic studies that certain segments of major faults rupture repeatedly, at fairly regular intervals, in similar-sized *characteristic* earthquakes (Schwarz & Coppersmith 1984; Bakun & McEvilly 1984). This implies that strong structural controls governing the nucleation and stopping of ruptures exist for extended time periods at particular localities along fault zones. Understanding the nature of these controls is clearly important from the viewpoint of hazard assessment, not only because they govern the size of characteristic earthquakes but also because it is the acceleration and deceleration of ruptures that radiates most of the high-frequency wave energy that induces strong ground motion (Madariaga 1983). Furthermore, there are indications that the structures responsible for rupture control may play additional roles in localizing hydrothermal fluid flow and magmatism at specific sites along lineaments.

This paper seeks to review our present understanding of the brittle infrastructure within *well-established* fault zones in relation to earthquake rupturing and other aspects of lineament behaviour. Attention is focused chiefly on deformation and seismic activity associated with transcurrent fault systems, notably the dextral San Andreas system, in part because many of the more conspicuous ancient lineaments are also of strike-slip character (see, for example, Bak *et al.* 1975; Jegouzo 1980) but mostly because of the high quality and quantity of regional seismological data available in California. Working on strike-slip faults has the additional advantage that structural irregularities transverse to the fault slip vector and to the generally horizontal direction of rupture propagation may be revealed by micro-earthquake epicentral distributions in map view. While similar fault complexity is to be expected in dip-slip systems, the infrastructure is then less easy to distinguish.

2. The seismogenic régime in continental crust

Improved seismograph coverage over the past several years, coupled with better location techniques, has led to the important conclusion that most continental earthquakes are restricted to the upper half of the crust (Meissner & Strehlau 1982; Sibson 1982; Chen & Molnar 1983). The background microseismicity in regions of active tectonism such as California is sufficiently high to define the base of what can be regarded as the *seismogenic régime* over comparatively short time periods. Along the major active strike-slip faults it typically extends to depths of 10–15 km, with larger fluctuations occurring locally (see, for example, Sanders & Kanamori 1984; Sibson 1984). There appears to be a crude inverse relation between values of regional conductive heat flow and the cut-out depth of this micro-earthquake activity, though other factors such as changes in crustal composition are also likely to play a role. Within the seismogenic régime, displacement along fault zones generally occurs by earthquake rupturing, though there are regions where aseismic slip is dominant (Sibson 1983). Larger shocks ($M_L > 5.5$) tend to nucleate towards the base of the seismogenic régime, with their ruptures extending laterally and upwards so that their aftershock sequences also are mostly confined to the same zone (figure 1).

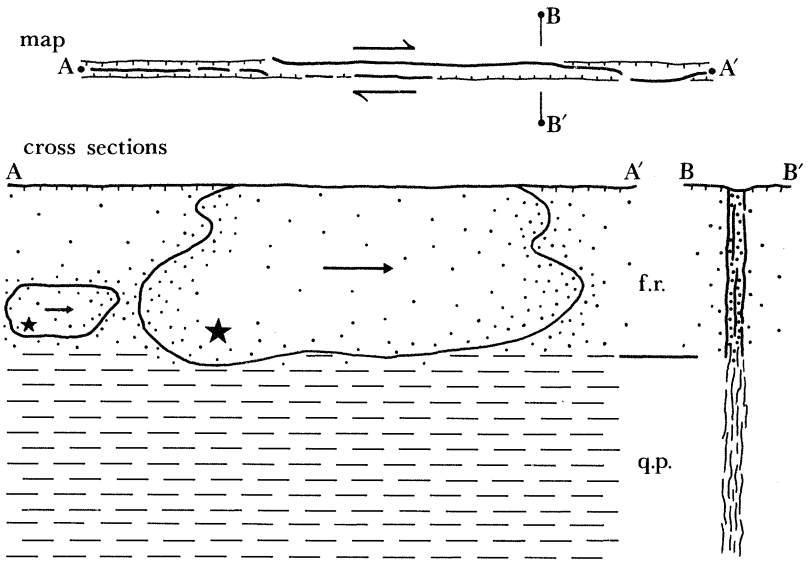

FIGURE 1. Schematic diagram of strike-slip earthquake faulting, illustrating the concept of the seismogenic régime. Segmented trace of principal slip surface in a major fault zone shown in map view. Sections show foci (stars) and rupture bounds of larger earthquakes with dots representing background micro-earthquakes and aftershocks. F.r. and q.p. refer to the frictional and quasi-plastic fault régimes, respectively.

The base of the seismogenic régime in quartzo-feldspathic crust has been interpreted as the transition from friction-dominant (f.r.) deformation to aseismic quasi-plastic (q.p.) shearing localized in mylonitic shear belts at depths below the onset of greenschist facies metamorphic conditions, reflecting the changing response of quartz to deviatoric stress once temperatures exceed *ca.* 300 °C (Sibson 1977, 1983). It is generally believed that high-level frictional deformation leading to seismic activity is driven by the localized aseismic shearing at depth (Thatcher 1975). Modelled profiles of shear resistance against depth suggest that the peak values of shear resistance and the greatest concentrations of distortional elastic strain energy should occur in the vicinity of the f.r.–q.p. transition, providing a rationale for the nucleation of larger earthquake ruptures around the base of the seismogenic zone.

Throughout the rest of this paper our main concern is with the infrastructure of transcurrent fault zones within the frictional seismogenic régime, though the likelihood that some of the high-level structural complexity is kinematically controlled by, or directly reflects, patterns of aseismic shearing at depth has to be borne in mind.

3. Infrastructure of fault zones in the seismogenic régime

Major active continental strike-slip fault zones with displacement of tens to hundreds of kilometres typically occupy prominent topographic furrows ranging in width from a few hundred metres to a kilometre or so (Kupfer 1960; Ambraseys 1970; Allen 1981). Often, they occur as the dominant strands in continental strike-slip fault systems extending laterally over distances of 100 km or more (Crowell 1974; Moore 1979). While permanent deformation related to the faulting such as echelon folding and subsidiary faulting (Wilcox *et al.* 1973; Aydin & Page 1984) may occur over a broad swathe, the most intense deformation and displacement appears to be restricted to these dominant fault zones. It seems likely that their near-surface

widths may reflect those of the driving mylonitic shear belts at mid-crustal depths which, from fossil examples, are typically of comparable scale (Jegouzo 1980; Sibson 1983).

Segmentation of the dominant fault zone may occur on a large scale. As a result of stepovers extending well beyond the characteristic width of the dominant fault zones, regions of localized contraction and extension associated respectively with restraining and releasing bends (Crowell 1974) may be interspersed with segments undergoing pure strike-slip (Aydin & Nur 1982, Mann *et al.* 1983). Our principal concern here, however, is the infrastructure within the dominant fault zones themselves. Interpretation of this infrastructure is generally hampered by poor exposure, but studies of recent rupture traces can be revealing, as can investigations of ancient exhumed transcurrent fault zones of comparable scale.

(*a*) *Existence of a principal slip surface*

Evidence from several sources suggests the presence within major fault zones of a principal slip surface (p.s.s.), often segmented or curved, which accommodates most of the displacement occurring seismically for extended time periods.

Finite deformation state

Studies relating macroscopic structure to finite rock deformation within ancient transcurrent fault zones now exposed at the brittle level are few. Perhaps the most detailed is that of Flinn (1977), who described fault geometry and deformation associated with the Walls Boundary Fault and related structures in Shetland. Excellent exposures of this transcurrent fault system (the probable northwards continuation of the Great Glen Fault) occur along the intricate coastline of the archipelago. Most of the faulting took place within the upper crust in a supra-greenschist metamorphic environment, with fault-related deformation affecting a wide range of sedimentary and crystalline rocks.

Several generalizations can be made. Cataclastic deformation associated with the Walls Boundary Fault is largely restricted to a sub-vertical dominant fault zone ranging up to *ca.* 1 km in width, though locally it may extend laterally for several kilometres. The intensity of deformation within the dominant fault zone is very heterogeneous both across and along strike, with different protoliths variably crushed, microfractured and chopped about by subsidiary faults to form largely random-fabric microbreccias and fault rocks of the cataclasite series. However, enclaves of comparatively underformed rock survive locally, often as fault-bounded slivers within regions of more intense deformation. The extent of hydrothermal alteration and veining, and of neomineralization within the main fault zone, are likewise highly variable.

Where exposure through the main fault zone is continuous, a single, dominant sub-vertical planar band of ultracataclasite-gouge less than 0.5 m in thickness can usually be recognized. Flinn (1977) argues convincingly that the bulk of the total strike-slip amounting to tens of kilometres has taken place across these zones of particularly intense grain-size reduction. This principal slip surface may be flanked on either side by breccia-cataclasite deformation for hundreds of metres, but more commonly defines one or other of the margins to the main fault zone. The presence of similar principal slip surfaces bounding broader regions of brittle deformation has been noted for the San Gabriel Fault of California (Anderson *et al.* 1983), for small strike-slip fault zones in the Sierra Nevada (Segall & Pollard 1983), and is also a common feature of the detachment faulting associated with the metamorphic core complexes of the western United States (Davis *et al.* 1980).

PHILOSOPHICAL TRANSACTIONS OF THE ROYAL SOCIETY A MATHEMATICAL, PHYSICAL & ENGINEERING SCIENCES

Broad and fine infrastructure revealed by strike-slip rupturing

The structural implications of selected strike-slip earthquake ruptures are discussed at length in §4. Here, the aim is to emphasize some general characteristics relevant to the gross infrastructure of the dominant fault zones. The existence of a complex and variable infrastructure may be inferred both from surface rupture patterns produced by individual earthquakes (see, for example, Tchalenko & Ambraseys 1970; Tchalenko & Berberian 1975), and from detailed maps recording patterns of ground breakage that probably result from a succession of recent events (see, for example, Vedder & Wallace 1970). Rupture complexity can usually be recognized over a range of cross-strike scales, of which two are dominant (figure 2). Individual rupture strands tend to exhibit an infrastructure which extends across strike for only 10 m or so. This fine infrastructure generally comprises en echelon Riedel shears and pressure ridges with occasional extension fissures (Tchalenko & Ambraseys 1970), all symptomatic of near-surface failure in a stress field kinematically induced by constrained planar slip at depth (Tchalenko 1970). Sharp (1979) cites field evidence suggesting that much of this fine infrastructure simplifies at a comparatively shallow depth to a single planar discontinuity.

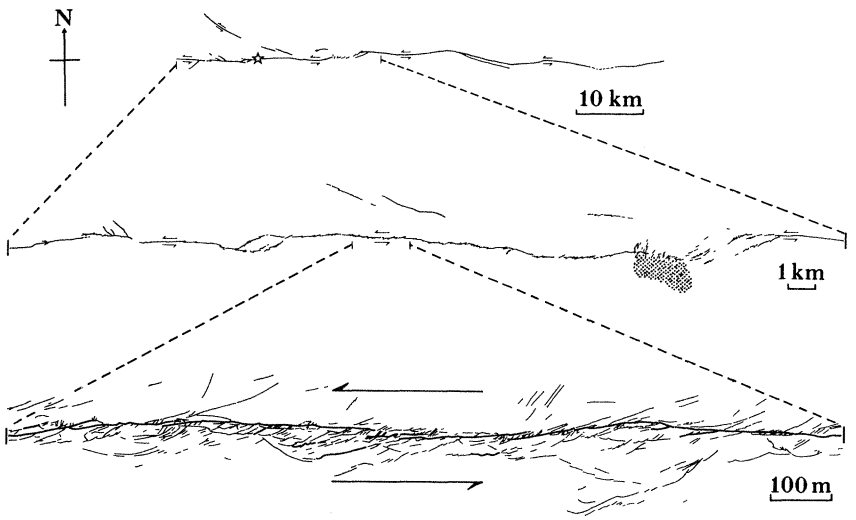

FIGURE 2. Left-lateral rupture trace from the 1968 Dasht-e-Bayaz earthquake in northern Iran, showing broad and fine-scale infrastructure (after Tchalenko & Ambraseys 1970; Tchalenko & Berberian 1975). Star indicates probable epicentre, stippling delineates area of intense sandblows.

Broader scale complexity appears related to the overall width of major fault zones, and is not so readily explicable in terms of simple shear kinematic control. Linear or gently curving individual rupture segments can rarely be followed for more than 10 km or so, suggesting that the largest strike-slip ruptures, extending for tens or hundreds of kilometres, are invariably multiple events (Wallace 1973). Slip then transfers across typical distances of 10^2–10^3 m to an echelon rupture segment. The step-sense of the echelon rupture segments is much less consistent than in the fine infrastructure. A close correlation sometimes exists between these stepover widths and the geomorphic expression of the dominant fault zone, suggesting that in at least some instances the principal slip surface is switching from one margin of the dominant fault zone to the other. Subsidiary fracturing is often intense in the stepover regions, but it is

comparatively rare for a principal rupture strand to curve continuously across such steps. An important additional point, to be emphasized later, is the demonstration by high-resolution microearthquake studies that infrastructure on this broader scale often extends throughout the seismogenic régime. Stepovers on this scale are also commonly associated with abrupt changes in the amount of slip accompanying individual earthquakes (Clark 1972; Tchalenko & Berberian 1975; Sieh 1978). It is rare for a major strike-slip displacement from an individual earthquake to extend across a stepover of more than a few kilometres, such as those associated with major rhombochasmic openings.

Analogy with experimental faulting

The preferential localization of principal slip surfaces at one or other of the boundaries to both ancient and active transcurrent fault zones invites comparison with the results of laboratory shearing experiments on layers of artificial quartz gouge sandwiched between intact rock (Engelder *et al.* 1975; Byerlee *et al.* 1978). While stable seismic shearing in these experiments takes place by localized or uniform cataclastic flow within the body of the gouge layer, intermittent stick-slip behaviour resembling natural earthquake rupturing occurs only along discrete surfaces at the gouge–rock interface.

(*b*) *Echelon segmentation and curvature of the principal slip surface*

Recent studies suggest that irregularities in the surface expression of the principal slip surface are often related to the epicentres, rupture bounds and patterns of aftershock activity associated with moderate to large earthquakes (Bakun *et al.* 1980; Segall & Pollard 1980). Two main types of irregularity, echelon steps and local bends, have been recognized within the broader infrastructure of transcurrent fault zones, each type occurring in two alternative asymmetries with respect to the overall sense of shear (figure 3).

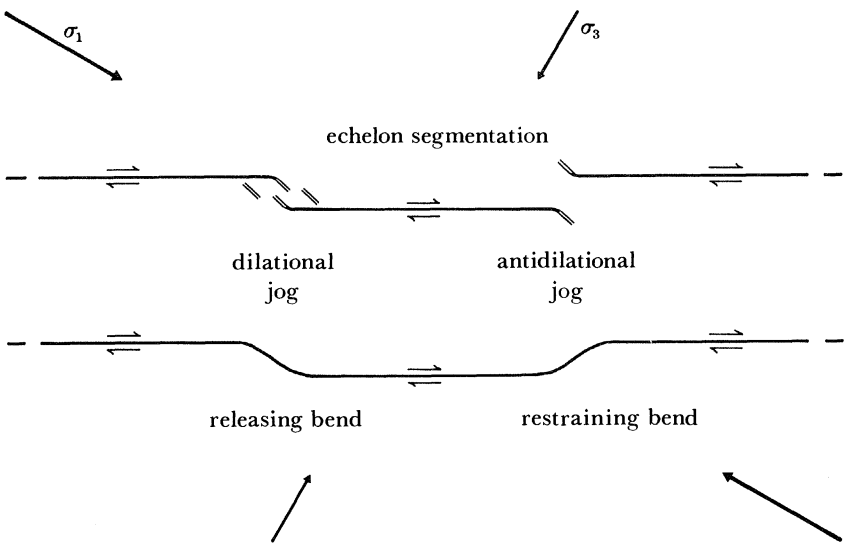

FIGURE 3. Echelon segmentation and curvature of the principal slip surface classified into dilational and antidilational fault jogs. Far-field principal compressive stresses, $\sigma_1 > \sigma_2$ (out of page) $> \sigma_3$. Short parallel lines denote likely extension fracture orientations.

Dilational and antidilational jogs

For ease of reference, irrespective of faulting mode or sense of shear, the alternative asymmetric forms for both types of irregularity can be classed as dilational or antidilational jogs depending on the tendency for areal increase or reduction, respectively, in the plane defined by the slip vector and the pole to planar segments of the principal slip surface. In a two-dimensional, quasi-static elastic analysis, Segall & Pollard (1980) examined stress-field perturbations arising from the alternate asymmetries of echelon segmentation, and their potential effects on fault behaviour. Fuller consideration will be given to the mechanical implications of this analysis in §5; at this stage it is appropriate to review only their main conclusions. For a dilational jog, the elastic interaction between fault segments decreases the frictional resistance at the segment tips, facilitating slip, and also lowers the mean compressive stress throughout the intersegment region, favouring the development of a linking extensional fracture system with subsidiary shearing. For an antidilational jog, however, both the frictional resistance at the segment tips and the mean compressive stress in the intersegment region increase, inhibiting slip transfer across the step and causing deformation to spread out over a broad area. Thus, on this quasi-static analysis, dilational jogs present no major impediment to the transfer of slip along a fault system, but antidilational jogs form potential locking points. Similar situations can be expected to arise when echelon linear traces of the principal slip surface are linked by curves, analogous to Crowell's (1974) concept on a larger scale of releasing and restraining bends (figure 3).

Origin of echelon segmentation

As noted previously, the lack of a consistent step-sense in the broader infrastructure is puzzling, and seems to preclude simple shear kinematic control of the kind envisaged for the fine infrastructure. Two possible explanations are as follows.

(i) The switching of the principal slip surface from one margin to the other of the main fault zone is somehow related to strain compatibility problems arising from the upward transfer into the discontinuous seismogenic régime of shear strain from a continuous mylonitic shear zone beneath (figure 1).

(ii) Mylonitic shear zones characteristically occur in a braided mesh pattern (Sibson 1977), and the high-level brittle infrastructure to some extent reflects the ductile shear zone mesh at depth.

(*c*) *Longevity of infrastructure*

A key question is for how long the infrastructure remains fixed in one configuration. Such limited data as we have are drawn almost entirely from geomorphological evidence. Analyses of progressively displaced flights of river terraces and other geomorphic features (see, for example, Lensen 1968; Sieh & Jahns 1984) have demonstrated that in at least some cases the trace of a principal slip surface within a major transcurrent fault zone remains fixed to less that 0.5 m for periods exceeding 10^4 years, during which time cumulative slip in excess of 100 m has occurred. The important consequence is that while incremental earthquake slip on echelon fault segments could conceivably be accommodated through stepover regions by elastic strain, the long-term transfer of these larger displacements inevitably requires permanent deformation localized in the vicinity of jogs.

PHILOSOPHICAL TRANSACTIONS OF THE ROYAL SOCIETY A MATHEMATICAL, PHYSICAL & ENGINEERING SCIENCES

(*d*) *Finite deformation associated with infrastructure*

From their geomorphic expression and from ancillary structures, it is clear that substantial permanent deformation is indeed sometimes associated with the broader infrastructure. Dilational jogs in the trace of the principal slip surface are often delineated by small pull-apart basins, while upwarping as a result of localized folding and thrusting may occur in the vicinity of antidilational jogs (figure 5). Available evidence suggests that jog structures on the scale of the dominant fault-zone width have often developed over periods in excess of 10^4 years (Freund 1971; Sharp & Clark 1972). The internal structure and mechanics of both kinds of jog, and the problems associated with incremental and large-slip transfer across them, are explored further in §5.

4. Earthquake rupturing, aftershock distributions and lineament infrastructure

In this section we consider some specific instances of earthquake rupture control within the San Andreas Fault System (figure 4). Information on the rupturing process is gleaned from surface rupture patterns, from both near-field and teleseismic waveform analyses, and from detailed studies of the distributions and focal mechanisms of aftershocks. We restrict our attention to moderate or greater ($M_L \geqslant 5.5$) dextral; strike-slip events that have occurred within the system over the past twenty years, and have been closely studied and documented.

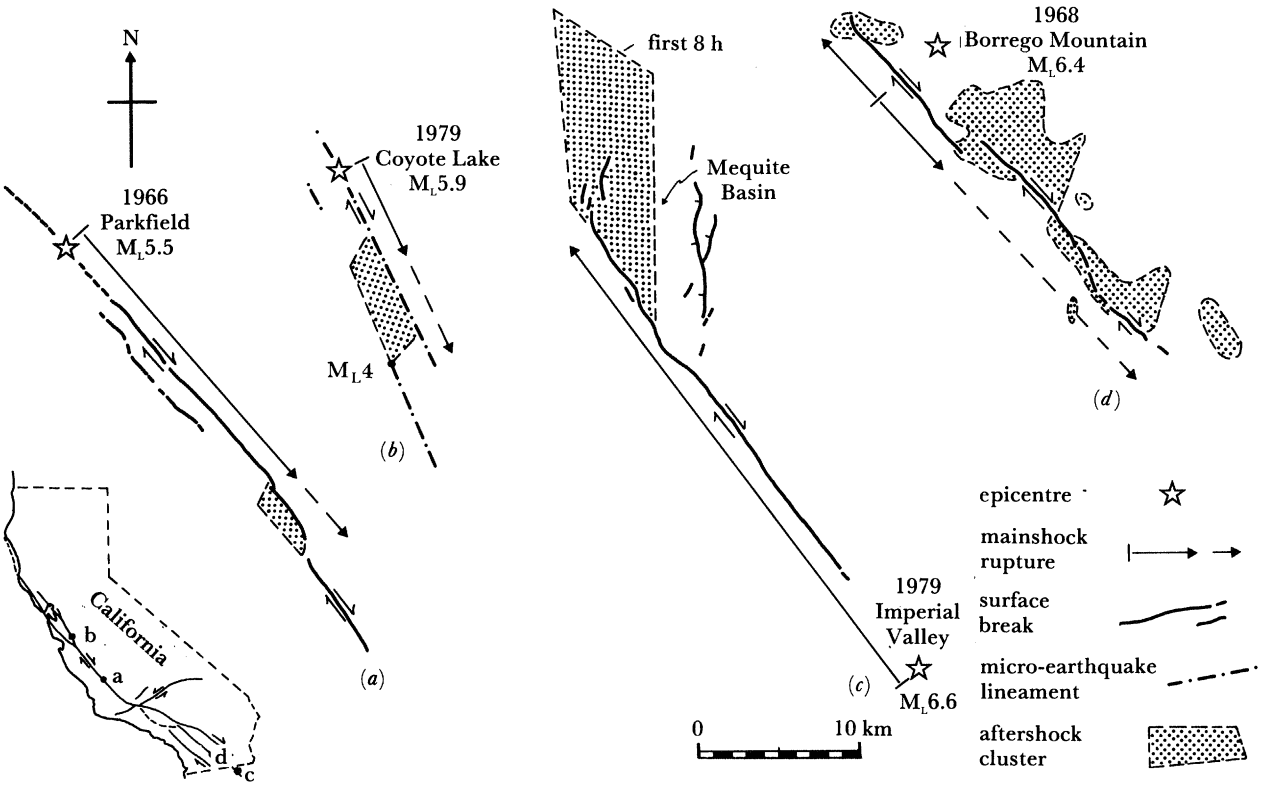

Figure 4. Seismotectonic cartoons of recent right-lateral strike-slip ruptures within the San Andreas Fault System.

(*c*) *Recent strike-slip ruptures within the San Andreas Fault System*

The 1965 M_L 5.5 *Parkfield earthquake*

This event is of particular interest as the latest in a series of characteristic $M_L \approx 5.5$ earthquakes that have previously ruptured the same Parkfield–Cholame segment of the San Andreas Fault. These occurred in 1934, 1922, 1901, 1881, and also possibly in 1857, as an immediate foreshock to the $M_L \approx 8$ earthquake that ruptured through the 'Big Bend' (Bakun & McEvilly 1984; Sieh 1978). Waveform analyses show that the last three events, at least, were virtually identical, with the implication of strong local controls on the nucleation, propagation, and stopping of these characteristic ruptures. Final ground breakage associated with the 1966 event extended for *ca.* 35 km (Brown *et al.* 1967) (figure 4*a*). Structurally significant features along the trace include a slight restraining bend (equivalent to an antidilational jog) associated with the epicentre, and a pronounced *ca.* 1 km dilational jog between echelon segments across the Cholame Valley. While dextral strike-slip at the surface eventually reached *ca.* 0.2 m near the centre of the rupture, most if not all of it developed by afterslip over a period of two months following the main shock (Smith & Wyss 1968). Aftershock epicentres were largely restricted to a narrow band less than 2 km in width and nearly coincident with the surface rupture trace. From this and the seismic strong-motion data, it has been argued that the main coseismic rupture was vertical, extended from 3 to 8 km in depth, and propagated unilaterally southeastwards for *ca.* 25 km from the epicentral bend, with a mean slip of 0.6 m, to terminate in the vicinity of the dilational jog (Lindh & Boore 1981). The surface fault break was discontinuous across the jog, but aftershock activity was particularly intense beneath a 3.5 km × 1 km rhomboidal area immediately northwest of its inferred position, indicating that the echelon segmentation persisted throughout the seismogenic régime to a depth of around 12 km. Focal mechanisms for most aftershocks were consistent with dextral strike-slip on sub-vertical planes parallel to the main rupture, but a component of normal dip-slip was evident for a few solutions within the dilational jog (Eaton *et al.* 1970). There are also indications of relative subsidence within this rhombic area over a period of weeks following the earthquake (Brown *et al.* 1967). The 8 km fault break extending southeast of the jog was probably entirely the product of post-mainstock afterslip, decreasing logarithmically with time along with the aftershock activity (Smith & Wyss 1968).

The 1979 M_L 5.9 *Coyote Lake earthquake*

Interpretations of rupture development during this earthquake on the Calaveras Fault (figure 4*b*) are based largely on high-precision aftershock studies and waveform analyses, because no clear surface break developed. However, the seismological data indicate remarkable similarities to the Parkfield earthquake, with the main rupture propagating unilaterally southeastwards to terminate adjacent to a dilational jog delineated by intense aftershock activity. Mainshock slip averaging *ca.* 0.2 m was largely confined to a sub-vertical rupture extending from 3 to 10 km in depth, which propagated southeastwards from the focus for 6–14 km (Bouchon 1982; Liu & Helmberger 1983). Some 5 h after the main earthquake, beginning with an M_L4.0 event, aftershock activity extended *ca.* 2 km southwest to an echelon fault segment and then migrated southeastward over a period of days to define a subsidiary slip plane 8 km in length at depths between 3 and 7 km (Reasenberg & Ellsworth 1982). Diffuse aftershock activity occurred within the overlap zone. Focal mechanisms obtained for aftershocks were almost uniformly consistent

PHILOSOPHICAL TRANSACTIONS OF THE ROYAL SOCIETY A MATHEMATICAL, PHYSICAL & ENGINEERING SCIENCES

with dextral strike-slip on sub-vertical planes parallel to the main rupture. However, within the dilational jog a clockwise swing of *ca.* 14° in the strike of probable fault planes was noted.

The 1979 M_L 6.6 *Imperial Valley earthquake*

Somewhat similar behaviour occurred during the 1979 M_L6.6 Imperial Valley earthquake, except that here the rupture propagated unilaterally northwestwards for *ca.* 35 km with an average coseismic slip of *ca.* 0.4 m, to terminate at a much larger scale dilational jog defined by the downthrown Mesquite Basin (figure 4*c*). Surface faulting occurred only on the northern three quarters of the rupture along the Imperial Fault, and also along the subsidiary Brawley Fault. Detailed analysis of the main rupture on the Imperial Fault (Archuleta 1984) shows that the amount of strike-slip, the slip rate, and the rupture velocity, all diminish abruptly north of the intersection with the Brawley Fault, but that the rupture continued on past a small restraining bend to stop finally where the strike of the Imperial Fault veers northwards. Logarithmically decaying horizontal afterslip was observed along the surface rupture of the Imperial Fault over a period of weeks after the earthquake, reaching maximum values in the centre of the trace (Harsh 1982). For the first 8 h after the main shock, aftershocks were almost entirely concentrated beneath a 7 km × 11 km rhombic area extending north from the main rupture termination, but some activity later spread along the main rupture (Johnson & Hutton 1982). It should be noted that the region extending northnorthwest as a strip from between the Imperial and Brawley Faults towards the southern termination of the San Andreas Fault (figure 4) is characterized by frequent micro-earthquake swarms and local geothermal activity, and appears to be a zone of crustal spreading (Weaver & Hill 1979).

The 1968 M_L 6.4 *Borrego Mountain earthquake*

The Borrego Mountain earthquake rupture on the Coyote Creek Fault within the San Jacinto Fault Zone appears rather more complex than the previous examples. Unfortunately only limited strong-motion data is available to constrain the rupture process. The surface break was mapped over a period of days after the main shock (Clark 1972). It extended a total distance of 31 km, but consisted of three distinct segments separated by antidilational and dilational jogs with stepovers of *ca.* 1.5 km (figure 4*d*). In the immediate vicinity of the antidilational jog Quaternary sediments have been substantially deformed into east–west trending folds, suggesting that the jog has been a long-term impediment to slip transfer along the fault (Sharp & Clark 1972). There are indications that the northern segment may also be terminating in a dilational jog at its northwestern extremity and that the southern segment may link through to the Superstition Mountain Fault by an antidilational job. Focal mechanism and aftershock studies suggest the main rupture plane dipped steeply (more than 80°) to the northeast (Allen & Nordquist 1972). Measured dextral strike-slip along the surface break reached a maximum value of *ca.* 0.38 m along the northern segment, with no significant afterslip apparent. Slip decreased to maximum values of *ca.* 0.27 m and *ca.* 0.11 m on the central and southern segments respectively, but in both cases this included extensive afterslip. On the central segment afterslip was observed shortly after the main shock, starting in the southeast close to the dilational jog but then extending over its entirety. On the southern segment its onset was delayed for perhaps a year (Clark 1972). The location of the focus for the main shock is consistent with rupture initiation at a depth of *ca.* 11 km in the centre of the northern fault segment, with possible bilateral rupture growth (Allen & Nordquist 1972). Subsequent detailed

waveform analyses (Burdick & Mellman 1976; Ebel & Helmberger 1982) suggest that the bulk of the radiated energy came from high-stress drop faulting localized in this same northern segment, with at most only a small contribution from the other rupture segments.

Aftershocks were well located at depths down to 12 km but were distributed over a broad region (Hamilton 1972). However, there appear to be some significant correlations with the surface rupture geometry. Epicentres for most of the aftershocks plot northeast of the rupture trace, at distances greater than can be attributed to location error or to the probable dip of the fault surface. Comparatively few were located in the immediate vicinity of the mainshock epicentre. The greatest concentration occurred northeast of the central segment with a pronounced cluster adjacent to the antidilational jog. From the Segall & Pollard (1980) analysis this corresponds to a region of reduced mean stress. While aftershock focal mechanisms were mostly consistent with strike-slip rupturing parallel to the main surface trace, a thrust component was locally evident in the vicinity of this jog. In contrast with the antidilational jog, most aftershocks in the vicinity of the southern dilational jog lay between the rupture segments. Southeastwards extension of activity along the southern rupture segment was noted a week after the main shock. Two distinct outlying clusters, which developed 15–20 km northeast and southwest from the main rupture zone, were attributed to off-fault increases in shear stress arising from the primary dislocation (Hamilton 1972). Minor activity also occurred along the trend of the rupture zone northwest of the mainshock.

(*b*) *Summary of rupture behaviour*

A number of significant points emerge from the preceding discussion.

(i) Deep infrastructure within major transcurrent fault zones can often be traced throughout the seismogenic zone by high-precision micro-earthquake studies and often reflects irregularities in surface rupture patterns.

(ii) Structural control of the rupture nucleation site is only obvious for the Parkfield earthquake, where the epicentre coincides with a small restraining bend.

(iii) There is good evidence for rupture arrest at specific structural sites. Three of the four ruptures considered in detail appear to have stopped at dilational jogs. However, in the case of the Borrego Mountain earthquake, southwards expansion of the main rupture was certainly impeded and possibly halted by an antidilational jog.

(iv) Where stopping occurs at a dilational jog, progressive extension of the aftershock zone along the echelon fault segment is often observed, suggesting time-dependent transfer of slip. Similar behaviour was associated with the southern, dilational jog along the Borrego Mountain rupture. Such delayed slip transfer seems to occur over a wide range of time scales.

(v) There is a marked contrast between the aftershock patterns associated with ruptures arrested at dilational and antidilational jogs. For ruptures stopped at a dilational jog, aftershock epicentres tend to lie along the primary rupture or its extensions, with distinctive rhomboidal concentrations, resembling swarm activity, associated with the jog. For the Borrego Mountain earthquake, where the initial rupture was at least partly arrested by an antidilational jog, aftershocks were asymmetrically distributed over a broad area, mostly to one side of the rupture trace. The greatest cluster occurred on the opposite side of the jog from the termination of the main rupture in a region where mean stress may be inferred to have diminished.

PHILOSOPHICAL TRANSACTIONS OF THE ROYAL SOCIETY A MATHEMATICAL, PHYSICAL & ENGINEERING SCIENCES

5. Internal structure and mechanics of jogs

From the foregoing discussion it appears that dilational jogs present at least as great an obstacle to the passage of earthquake ruptures as antidilational jogs. This is contrary to the prognosis from Segall & Pollard's (1980) quasi-static analysis of the elastic interaction between echelon fault segments, suggesting that slip transfer across jogs may be additionally complicated by dynamic effects. Another point to be considered is the possible role of fluid pressure in jog behaviour. Throughout the seismogenic régime, background fluid pressures within fault zones are probably at hydrostatic levels or greater, increasing downwards at greater than or equal to 10 MPa km^{-1} (Sibson 1981). Seismic activity can be affected by changes in fluid pressure (Raleigh *et al.* 1972), and in turn, large earthquakes may locally perturb fluid pressures (Nur & Booker 1972). In the upper few kilometres of the crust, at least, the frictional strength of faults appears to be adequately described by a simple failure criterion of Coulomb form:

$$\tau = C + \mu_s (\sigma_n - P), \tag{1}$$

where τ and σ_n are respectively the shear and normal stresses on the fault, P, is the fluid pressure and C is the cohesive strength (which may be rather low); and the coefficient of static friction, μ_s, typically has a value of *ca.* 0.75 (Sibson 1983). Seismic activity may therefore be triggered by increases in fluid pressure as well as by increased deviatoric stress. Conversely, faults will be strengthened by a decrease in fluid pressure.

To examine the manner in which propagating ruptures may interact with fault jogs, we first need to consider their probable internal configuration.

(*a*) *Internal structure*

The infrastructure of fault jogs may be considered with regard to both their incremental and their long-term development. Information on incremental structural development comes from theoretical and experimental fracture mechanics, and from the character of jog-related seismicity. Clues as to their long-term evolution come from the geomorphic expression of active jogs and from associated finite deformation. Comparative analyses of small-scale fault jogs are useful in both regards. Likely structural configurations within major fault jogs are summarized in figure 5.

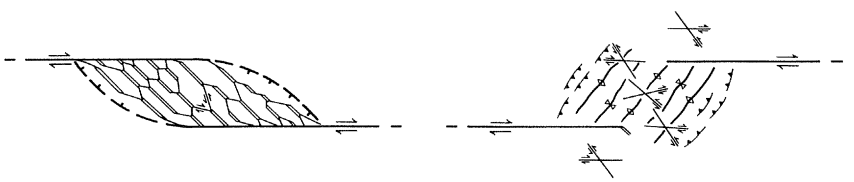

Figure 5. Synoptic map views of probable internal structure within dilational and antidilational fault jogs on a transcurrent fault. Extension fractures represented by parallel lines, subsidiary conjugate strike-slip faults by thin criss-cross lines, normal faults by broken lines with tick on downthrown side, thrusts by sawtooth lines, and fold axial traces by thick wavy lines.

Infrastructure of dilational jogs

The surface expression of dilational fault jogs is often characterized by depressed areas taking the form of elongate rhomboidal basins contained within the main fault zone. In some cases, these depressions are sharply bounded by normal faults splaying off the strike-slip faults; in others the boundaries are obscured by marginal slumping (Freund 1971; Mann *et al.* 1983). However, given the dimensions and aspect ratios of these depressions, it seems implausible that the bounding normal faults are dominant structural components throughout the seismogenic régime. Furthermore, in the examples considered previously, aftershock activity within the dilational jogs yielded a preponderance of strike-slip focal mechanisms, with a component of normal slip evident only in a few instances. Note also that most related seismicity occurred in a diffuse band between the echelon strike-slip segments, indicating strong localization of the deformation related to slip transfer.

Another important consideration is the strong tendency, demonstrable theoretically and experimentally, for echelon fault segments in this configuration to propagate into and become linked by extension cracks aligned perpendicular to the least principal compressive stress (figures 3, 5) (Brace & Bombolakis 1963; Segall & Pollard 1980). This tendency has also been widely observed in dilational jogs described on a range of scales from ancient fault zones (Spurr 1925; Gamond 1983; Segall & Pollard 1983). Echelon planar fault segments tend to be linked through the jogs by individual or multiple extension fractures, occasionally with subsidiary shears, or by the development of more extensive rhombic or lensoidal openings. The linking fractures are commonly infilled either by hydrothermal mineralization (quartz and calcite dominate) forming extension veins of massive, crustiform or fibrous habit, or by breccias of wallrock fragments cemented by hydrothermal minerals. In many cases, textural evidence suggests a history of incremental opening for the extension veins, or of multi-episode brecciation and recementation (Hulin 1925; Mitchell 1974). While they are clearly fault-related, the low clast : matrix ratios of these recemented breccias indicate significant dilation with included clasts of wallrock remaining angular and showing little evidence for an origin by frictional attrition (Phillips 1972). The important geometrical conclusion, however, is that the total extensional opening across the linking fracture system in the direction of fault movement is generally comparable to the slip on the echelon fault segments.

The association of high *b*-value swarm seismicity with active large-scale dilational jogs in the San Andreas Fault System led Weaver & Hill (1979) to propose an infrastructure of short conjugate strike-slip shears linked by vertical extension fractures into a honeycomb mesh. This model, perhaps with some additional complexities from local normal slip faulting, accounts satisfactorily for most observed characteristics of dilational jogs, and forms the basis of our interpretation of their infrastructure (figure 5).

(*b*) *Infrastructure of antidilational jogs*

Theory, experiments, and field observations demonstrate the tendency for the tips of echelon fault segments in antidilational jogs to diverge away from each other into extension fractures (figure 3). However, the regions of possible tensile failure are small, and development of subsidiary strike-slip faulting in a swathe linking and extending beyond the segment tips is more highly favoured (Segall & Pollard 1980). For the antidilational jog associated with the Borrego Mountain rupture this is borne out by aftershock focal mechanisms, which show that strike-slip

faulting is dominant throughout the seismogenic régime with only minor thrusting. However, the difficulty of long-term slip transfer across the jog is manifested at the surface by extensive folding and localized updoming in the vicinity of the jog (figure 5).

(*b*) *Fluid flow and time-dependent behaviour*

An important mechanical distinction between dilational and antidilational jogs can be made on the basis of their probable internal configurations (figure 5). Whereas slip transfer across an antidilational jog is accomplished largely by subsidiary faulting, slip transfer across a dilational jog additionally requires substantial opening of extension fractures. This provides an explanation for the frequently observed time-dependence of slip transfer across dilational jogs. The time-dependent behaviour arises from the difficulty in opening linking extension fractures within fluid-saturated crust over periods comparable to earthquake rise-times of 1–10 s (Sibson 1985). Such rapid opening of extension fractures is strongly opposed by suctional forces arising from induced fluid pressure differentials, which may approach initial hydrostatic values at any depth. Hydraulic implosion of wallrock into the fractures may occur as a result of these fluid pressure differences, giving rise to the high-dilation breccias often found in fossil dilational jogs (Mitchell 1974). Furthermore, drops in fluid pressure that occur within the jogs from incipient extensional opening compound the problems of slip transfer by strengthening subsidiary faults. Resistive forces scale with the width of the jogs. If the larger (*ca.* 1 km wide) jogs are taken to extend through the seismogenic régime, the energy required for rapid slip transfer against induced suctions is comparable with the wave energy radiated by moderate or larger earthquakes.

Dilational jogs are therefore formidable barriers to the rapid transfer of slip. However, once a rupture has been arrested at a dilational jog, concentrations of strain energy at its termination may be slowly dissipated by delayed slip transfer with concomitant aftershock migration, as fluid pressures re-equilibrate by diffusion to allow the necessary extensional opening within linking fracture systems. The range of possible fluid diffusivities in the wallrock is sufficient to permit large variations in the rate of slip transfer, as indeed is observed. Control of aftershock activity by fluid diffusion has previously been considered by Nur & Booker (1972), but not at such specific sites.

(*c*) *Incremental versus finite slip transfer*

Dilational and antidilational jogs therefore present some interesting contrasts in behaviour with regard to rapid and long-term slip transfer. Both types of jog may impede earthquake ruptures and lead to their partial or complete arrest. However, the possibility of delayed slip transfer across dilational jogs suggests they represent no long-term impediment to fault motion in accordance with the quasi-static analysis of Segall & Pollard (1980), and field evidence indicates they may often be long-lived features of fault zones (Mann *et al.* 1983). In contrast, antidilational jogs form barriers to both incremental and long-term slip transfer. In view of this, one may speculate that they tend to be comparatively short-lived structures that have to be bypassed for large displacements to be accommodated.

PHILOSOPHICAL TRANSACTIONS OF THE ROYAL SOCIETY A MATHEMATICAL, PHYSICAL & ENGINEERING SCIENCES

6. Implications for mineralization and magmatism

The stopping or perturbation of earthquake ruptures by both kinds of fault jog, and the contrasting aftershock distributions that ensue (figure 6), have interesting implications for the localization of hydrothermal fluid flow, mineralization and magmatism along transcurrent lineaments. Intense micro-earthquake activity can clearly be expected to result in substantial cataclastic deformation and enhanced fracture permeability, though such permeability may be transitory as a consequence of hydrothermal self-sealing (Sibson 1981). However, as previously discussed, there may also be a direct cause-and-effect relation between fluid flow and aftershock activity. Nur & Booker (1972) attribute the time-dependent decay of aftershocks to the diffusion of aqueous fluids between zones of raised and lowered mean stress at rupture terminations. In their model, changes in fluid pressure immediately following the main shock reflect changes in mean stress, with fluids then migrating towards the zones of reduced mean stress. As fluid pressures within these zones increase back to their pre-mainshock values, shear failure is induced locally in accordance with (1), giving rise to aftershocks.

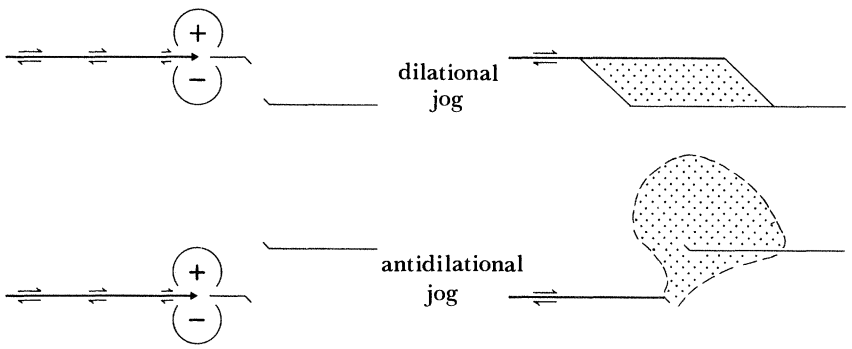

Figure 6. Schematic representation of ruptures terminating at dilational and antidilational fault jogs to produce contrasting aftershock distributions. Fields of compression (+) and dilation (−) at the rupture tips are indicated.

For both dilational and antidilational jogs the main aftershock concentrations do indeed seem to be occurring in regions where, according to the Segall & Pollard (1980) analysis, mean stress should be lowered as a result of elastic interaction between the echelon fault segments. For rupture arrest at an antidilational jog, an extensive area of reduced mean stress may lie well outside the main fault zone (cf. the patchy cataclastic deformation extending laterally from the Walls Boundary fault in §3.1). Intermittent flow of hydrothermal fluids into such aftershock regions following successive major earthquakes could well give rise to ill-defined, disseminated mineralization.

In contrast, dilational jogs potentially form optimal sites for concentrated hydrothermal mineralization. This is especially so in regions of igneous activity where intrusive dike swarms may be restricted to the local extensional régimes within such jogs. The opening of extension fracture systems attendant on earthquake rupture arrest and the resulting abrupt drops in fluid pressure present particularly favourable circumstances for rapid mineral deposition in vein stockworks and implosion breccias (Sharp 1965; Mitchell 1974). Note that the driving fault segments themselves may remain as comparatively barren, inconspicuous features near the

boundaries of the mineralized fracture systems. The southern termination of the San Andreas Fault is a current setting where recent magmatism and geothermal activity involving metalliferous brines are concentrated in dilational fault jogs (Weaver & Hill 1979). It is interesting to speculate on the consequences for hydrothermal deposition of a major earthquake rupture terminating in such structures.

These concepts of mineralization related to fault jogs are, of course, applicable to other modes of fault slip. In the general case of oblique slip, the jog structures will tend to occur as linear features confined within the enveloping surfaces of the fault zone and oriented perpendicular to the slip vector. Mineralization in dilational fault jogs appears to be especially common along faults with a large normal slip component in magmatically active extensional régimes (Newhouse 1942; McKinstry 1948).

7. Conclusions

Within the seismogenic régime where fault displacements are accommodated largely by earthquake rupturing, it is evident that the brittle infrastructure of fault lineaments exerts major controls, not only on rupture development but also on related processes such as fluid flow. To comprehend these controls fully, it is necessary to consider the *dynamic* interactions between propagating ruptures and the different varieties of fault infrastructure, such as dilational and antidilational jogs, in fluid-saturated crust. At present, we are at an early stage in understanding the complexities of these interactions, but it is already apparent that the interplay of processes has important ramifications for rupture perturbation and arrest, aftershock activity and fault-related mineralization.

This paper is dedicated to the memory of Professor Janet Watson, F.R.S. Support for the research was provided by the National Science Foundation.

References

Allen, C. R. 1981 In *The modern San Andreas fault* (ed. W. G. Ernst), pp. 51–534. New Jersey: Prentice-Hall.
Allen, C. R. & Nordquist, J. M. 1972 *U.S. Geol. Surv. Prof. Pap.* 787, pp. 16–23.
Ambraseys, N. N. 1970 *Tectonophysics* **9**, 143–165.
Anderson, J. L., Osborne, R. H. & Palmer, D. F. 1983 *Tectonophysics* **98**, 209–251.
Archuleta, R. J. 1984 *J. Geophys. Res.* **89**, 4559–4585.
Aydin, A. & Nur, A. 1982 *Tectonics* **1**, 91–106.
Aydin, A. & Page, B. M. 1984 *Bull. geol. Soc. Am.* **95**, 1303–1317.
Bak, J., Grocott, J., Korstgard, J. A., Sorenson, K., Nash, D. F. & Watterson, J. 1975 *Nature, Lond.* **254**, 566–569.
Bakun, W. H., Stewart, R. M., Bufe, C. G. & Marks, S. M. 1980 *Bull. seismol. Soc. Am.* **70**, 185–201.
Bakun, W. H. & McEvilly, T. V. 1984 *J. geophys. Res.* **89**, 3051–3058.
Berberian, M., Jackson, J. A., Ghorashi, M. & Kadjar, M. H. 1984 *Geophys. J. R. astr. Soc.* **77**, 809–838.
Bouchon, M. 1982 *Bull. seismol. Soc. Am.* **72**, 745–757.
Brace, W. F. & Bombolakis, E. G. 1963 *J. geophys. Res.* **68**, 3709–3713.
Brown, R. D. 1970 *U.S. Geol. Surv. Misc. Geol. Invest. Map* 1-575, scale 1:63500.
Brown, R. D., Vedder, J. G., Wallace, R. E., Roth, E. F., Yerkes, R. F., Castle, R. O., Waanen, A. O., Page, R. W. & Eaton, J. P. 1967 *U.S. Geol. Surv. Prof. Pap.* 579, pp. 1–66.
Buckland, W. 1836 *Geology and mineralogy with reference to natural theology*. London: William Pickering.
Burdick, L. J. & Mellman, G. R. 1976 *Bull. seismol. Soc. Am.* **66**, 1485–1499.
Byerlee, J., Mjachkin, V., Summers, R. & Voevoda, O. 1978 *Tectonophysics* **44**, 161–171.
Chen, W. P. & Molnar, P. 1983 *J. Geophys. Res.* **88**, 4183–4214.
Clark, M. M. 1972 *U.S. Geol. Surv. Prof. Pap.* 787, pp. 55–86.
Crowell, J. C. 1974 *Soc. Econ. Paleo. & Mineral. Spec. Publ.* 22, pp. 190–204.
Das, S. & Aki, K. 1977 *J. geophys. Res.* **82**, 5658–5670.

Davis, G. A., Anderson, J. L., Frost, E. G. & Shackelford, T. J. 1980 *Geol. Soc. Am. Mem.* **153**, 70–129.
Deng, Q. & Zhang, P. 1984 *J. geophys. Res.* **89**, 5699–5710.
Eaton, J. P., O'Neill, M. E. & Murdock, J. N. 1970 *Bull. seismol. Soc. Am.* **60**, 1151–1197.
Ebel, J. E. & Helmberger, D. V. 1982 *Bull. seismol. Soc. Am.* **72**, 413–437.
Engelder, J. T., Logan, J. M. & Handin, J. 1975 *Pur. appl. Geophys.* **113**, 69–86.
Flinn, D. 1977 *J. geol. Soc. Lond.* **133**, 231–248.
Freund, R. 1971 *N.Z. Geol. Surv. Bull.* **86**, 1–49.
Gamond, J. F. 1983 *J. struct. Geol.* **5**, 33–46.
Gay, N. C. & Ortlepp, W. D. 1979 *Bull. geol. Soc. Am.* **90**, 47–58.
Hamilton, R. M. 1972 *U.S. Geol. Surv. Prof. Pap.* 787, pp. 31–54.
Hanks, T. C. 1979 *J. geophys. Res.* **84**, 2235–2242.
Harsh, P. W. 1982 *U.S. Geol. Surv. Prof. Pap.* 1254, pp. 193–203.
Hulin, C. D. 1929 *Econ. Geol.* **24**, 15–49.
Jegouzo, P. 1980 *J. struct. Geol.* **2**, 39–47.
Johnson, C. E. & Hutton, L. K. 1982 *U.S. Geol. Surv. Prof. Pap.* 1254, pp. 59–76.
Kanamori, H. 1978 *U.S. Geol. Surv. Open-file Report* 78–380, pp. 283–318.
Kanamori, H. & Stewart, G. S. 1978 *J. geophys. Res.* **83**, 3427–3434.
Kupfer, D. H. 1960 *N.Z. Jl. Geol. Geophys.* **7**, 685–701.
Lee, W. H. K. & Stewart, S. W. 1981 *Principles and Applications of microearthquake networks*. Princeton: Academic Press.
Lensen, G. J. 1968 *Bull. geol. Soc. Am.* **79**, 545–556.
Lindh, A. G. & Boore, D. M. 1981 *Bull. seismol. Soc. Am.* **71**, 95–116.
Liu, H-L. & Helmberger, D. V. 1983 *Bull. seismol. Soc. Am.* **73**, 201–218.
Madariaga, R. 1983 *Ann. Geophys.* **1**, 17–23.
Mann, P., Hempton, M. R., Bradley, D. C. & Burke, K. 1983 *J. Geol.* **91**, 529–554.
McGarr, A. 1981 *J. geophys. Res.* **86**, 3901–3912.
McKinstry, H. E. 1948 *Mining geology*. New Jersey: Prentice-Hall.
Meissner, R. & Strehlau, J. 1982 *Tectonics* **1**, 73–89.
Mitchell, T. W. 1974 *Econ. Geol.* **69**, 412–413.
Moore, J. M. 1979 *J. geol. Soc. Lond.* **136**, 441–454.
Newhouse, W. H. 1942 *Ore deposits as related to structural features*. Princeton: University Press.
Nur, A. & Booker, J. R. 1972 *Science, Wash.* **175**, 885–887.
Nur, A. & Israel, M. 1980 *Phys. Earth planet. Inter.* **21**, 225–236.
Phillips, W. J. 1972 *J. geol. Soc. Lond.* **128**, 337–360.
Raleigh, C. B., Healy, J. H. & Bredehoeft, J. D. 1972 *Am. Geophys. Union Mon.* **16**, 275–284.
Reasenberg, P. & Ellsworth, W. L. 1982 *J. geophys. Res.* **87**, 10637–10655.
Rudnicki, J. W. & Kanamori, H. 1981 *J. geophys. Res.* **86**, 1785–1793.
Sanders, C. O. & Kanamori, H. 1984 *J. geophys. Res.* **89**, 5873–5890.
Schwartz, D. P. & Coppersmith, K. J. 1984 *J. geophys. Res.* **89**, 5681–5698.
Segall, P. & Pollard, D. D. 1980 *J. geophys. Res.* **85**, 4337–4350.
Segall, P. & Pollard, D. D. 1983 *J. geophys. Res.* **88**, 555–568.
Sharp, R. V. 1979 *U.S. Geol. Surv. Open-file Report* 79-1239, pp. 66–78.
Sharp, R. V. & Clark, M. M. 1972 *U.S. Geol. Surv. Prof. Pap.* 787, pp. 131–140.
Sharp, W. E. 1965 *Econ. Geol.* **60**, 1635–1644.
Sibson, R. H. 1977 *J. geol. Soc. Lond.* **133**, 191–214.
Sibson, R. H. 1981 In *Earthquake prediction: an international review* (ed. D. W. Simpson & P. G. Richards), pp. 593–603. Am. Geophys. Union Maurice Ewing Series 4.
Sibson, R. H. 1982 *Bull. seismol. Soc. Am.* **72**, 151–163.
Sibson, R. H. 1983 *J. geol. Soc. Lond.* **140**, 741–767.
Sibson, R. H. 1984 *J. geophys. Res.* **89**, 5791–5799.
Sibson, R. H. 1985 *Nature, Lond.* **316**, 248–251.
Sieh, K. E. 1978 *Bull. seismol. Soc. Am.* **68**, 1421–1448.
Sieh, K. E. & Jahns, R. H. 1984 *Bull. geol. Soc. Am.* **95**, 883–896.
Smith, S. W. & Wyss, M. 1968 *Bull. seismol. Soc. Am.* **58**, 1955–1973.
Spurr, J. E. 1925 *Econ. Geol.* **20**, 115–152.
Tchalenko, J. S. 1970 *Bull. geol. Soc. Am.* **81**, 1625–1640.
Tchalenko, J. S. & Ambraseys, N. N. 1970 *Bull. geol. Soc. Am.* **81**, 41–60.
Tchalenko, J. S. & Berberian, M. 1975 *Bull. geol. Soc. Am.* **86**, 703–709.
Thatcher, W. 1975 *J. geophys. Res.* **80**, 4862–4872.
Vedder, J. G. & Wallace, R. E. 1970 *U.S. Geol. Surv. Misc. Invest. Map* 1-574, scale 1:24000.
Wallace, R. E. 1973 In *Proceedings of the conference on tectonic problems of the San Andreas fault system* (ed. R. L. Kovach & A. Nur), pp. 248–250. Stanford Univ. Spec. Publ. Geol. Sci. xiii.
Weaver, C. S. & Hill, D. P. 1979 *Pure appl. Geophys.* **17**, 51–64.
Wilcox, R. E., Harding, T. P. & Seely, D. R. 1973 *Bull. Am. Assoc. petrol. Geol.* **57**, 74–96.

PHILOSOPHICAL TRANSACTIONS OF THE ROYAL SOCIETY A MATHEMATICAL, PHYSICAL & ENGINEERING SCIENCES